PROCEEDINGS, Thirtieth Workshop on Geothermal Reservoir Engineering
Stanford University, Stanford, California, January 31-February 2, 2005
SGP-TR-176

LATTICE BOLTZMANN SIMULATION OF FLUID FLOW IN SYNTHETIC FRACTURES

Erdinc Eker and Serhat Akin

Middle East Technical University
Department of Petroleum and Natural Gas Engineering
Ankara, 06531 TURKEY
e-mail:serhat@metu.edu.tr

ABSTRACT

Fractures play an important role in geothermal reservoir engineering as they dominate the fluid flow in the reservoir. Because of this reason determination of fracture permeability is very important to predict the performance of the geothermal reservoir. A fracture is usually assumed as a set of smooth parallel plates separated by a constant width. The absolute permeability of a smooth-walled fracture is related to the fracture aperture using the cubic law. However, the flow characteristics of an actual fracture surface would be quite different, affected by tortuousity and surface roughness. Though several researchers have discussed the effect of friction on flow, a unified methodology for studying flow on a rough fracture surface has not emerged. As experimental methods are expensive and time consuming most of the time numerical methods are used. In this work, we present results of the numerical computations for single phase flow simulations through two-dimensional synthetically created fracture apertures. These synthetic rock fractures are created using different fractal dimensions, anisotropy factors, and mismatch lengths that are obtained from the producing geothermal reservoirs in South Western Turkey. Lattice Boltzmann Method, which is a new computational approach suitable to simulate fluid flow especially in complex geometries, was then used to determine the permeability for different fractures. Regions of high velocity and low velocity flow were identified. The resulting permeability values were less than the ones obtained with the cubic law estimates. It has been found that as the mean aperture-fractal dimension ratio increased permeability increased. Moreover as the anisotropy factor increased permeability decreased with a second order polynomial relationship.

1 INTRODUCTION

The problem of modeling and simulating fluid flow in porous media always remained as the major research subject in reservoir engineering. Petrophysical properties of the reservoir rocks must be realistic and accurate for reservoir simulation works. One of the most important properties of the reservoir rock is the permeability, which is defined as the measure of the capacity of the medium to transmit fluids (Amyx, *et al*, 1960). The ability of a fracture to conduct a fluid when the saturation of that fluid is 100 percent of the space is known as the absolute permeability of that fracture to that fluid. The effective permeability of the fracture to the fluid is the permeability when the fluid has a saturation of less than a 100 percent. Researchers beginning with Lomize (1951), Snow (1965), Louis (1969), Bear (1972), Witherspoon *et al* (1980) and Golf-Racht (1982) studied the permeability of single-phase flow in fractures extensively. They have all shown that for steady state, isothermal, laminar flow between parallel glass plates the absolute permeability is a function of fracture spacing, *b*, and is given by the following equation:

$$k_{abs} = \frac{b^2}{12} \tag{1}$$

But as this equation does not represent the surface roughness of the real fractures a modification should be performed to consider the effect of surface roughness to the fracture permeability (Witherspoon *et al*, 1980):

$$k_{abs} = \frac{b^2}{(12\,f)} \tag{2}$$

Where *f* is defined as the surface roughness factor.

Accurate representation of fracture permeability is still a challenging research topic in reservoir engineering. In order to tackle this problem the use of lattice Boltzmann method is proposed (McNamara and Zanetti, 1988). In this work, by using the lattice Boltzmann method two dimensional fluid flows in synthetically created realistic fractures were simulated. Fracture fractal dimensions of some geothermal fields located in Turkey were used to create synthetic fractures using a fractal approach. The results were compared with the aforementioned empirical equations. The paper is organized as follows: in Section 2 the theory of synthetic fracture generation and lattice Boltzmann method is introduced. In Section 3 the process of synthetic fracture generation and the usage of these fractures in lattice Boltzmann simulation are described. Section 4 presents the results of the lattice Boltzmann simulation and comparison with other techniques. Finally, in Section 5 the main conclusions of this study are outlined.

2 BACKGROUND

In this section, theory of the lattice Boltzmann method is presented and compared with other numerical simulation techniques. Then, the concept of synthetic fractures and their reliability for defining the real fractures are described.

2.1 Lattice Boltzmann Method

Before giving the details of the method Cellular Automata theory will be given as it is the basis for lattice Boltzmann method.

Cellular automata theory

Cellular Automata (CA) are discrete dynamical systems whose behavior is completely specified in terms of local relations. They are mathematical models for complex natural systems containing large numbers of simple identical components with local interactions (Wolfram, 1984). Cellular Automata can be characterized as follows (Wolf-Gladrow, 2000):

- CA is regular arrangements of single cells of the same kind.
- Each cell holds a finite number of discrete states.
- The states are updated simultaneously at discrete time levels.
- The update rules are deterministic and uniform in space and time.
- The rules for the evolution of a cell depend only on a local neighborhood of cells around it.

CA is valuable because of its capability to display complex behavior by using the simple update rules. This property makes CA a strong candidate for the simulation tool for the physical phenomena like fluid flow. As it is stated in Ilachinski (2001) the most successful practical application of CA as *computing* devices is in the field of fluid mechanics. Despite still being in their infancy, CA models of fluid dynamics have already demonstrated that they can reproduce many of the essential features of thermodynamical and hydrodynamical behavior. This capability of CA is proved by Frisch *et al* (1986). They stated that a simple CA obeying nothing but conservation laws at microscopic level was able to reproduce the complexity of real fluid flows and named it as "Lattice Gas Automata (LGA)".

Lattice gas automata belong to a special class of CA designed to study various physical systems. Lattice Boltzmann method (LBM), which is used in our work, was developed by McNamara and Zanetti (1988) in response to the drawbacks of the lattice gas automata method. The main difference between two methods is that LBM describes the particle density as a continuous function instead of a Boolean variable. Moreover, LBM reduces the statistical noise produced by the Boolean arithmetic of the lattice gas automata.

Principles of the Lattice Boltzmann method

LBM as all other CA based methods that simulate natural phenomena like fluid flow uses an approach that is different from the conventional methods. This approach is named as "*bottom-up*" approach and is totally different from the techniques such as the "finite-element" and "finite-difference" methods. Figure 1 (Wolf-Gladrow, 2000) shows the difference between two methods.

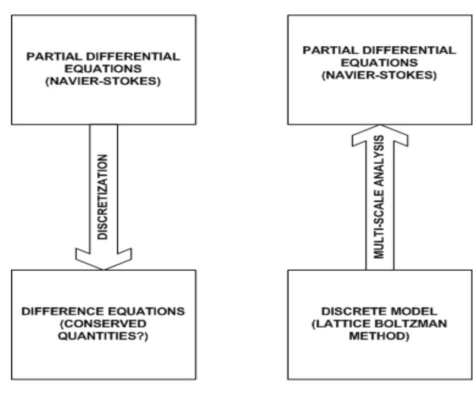

Figure 1. Difference between top-down and bottom-up approach (After Wolf-Gladrow, 2000).

In traditional methods (top-down approach) normally partial differential equations (PDEs) are used to simulate fluid flow. These PDEs are discretized by finite differences, finite volumes or finite elements. The resulting algebraic equations or systems of ordinary differential equations are solved by standard numerical methods. As for numerical simulations, conventional highly nonlinear Navier-Stokes equations are solved for both porous and fractured media. Numerical simulations have serious drawbacks like long computation times, poor convergence and numerical instabilities.

LBM is developed as another computational method that is more efficient and it uses simple rules to represent the fluid flow rather than partial differential equations. LBM is a discrete computational method based upon the Boltzmann equation. It considers a typical volume element of fluid to be composed of a collection of particles that are represented by a particle velocity distribution function at each grid point. In discrete time steps the fluid particles can collide with each other as they move. The rules that govern the collisions of the particles are designed such that the time averaged motion of the particles is consistent with the Navier-Stokes equation. One of the most important advantages of the LBM is its capability for handling fluid flow especially in complex geometries (Succi *et al*, 1989). The complex geometric details in the porous media and fractures can be handled in terms of simple bounce-back rules. Moreover, LBM could be applied to both two and three dimensional flows.

2D Lattice Boltzmann BGK model

In our work two-dimensional Bhatnagar-Gross-Krook (BGK) Lattice Boltzmann method is used. This model uses a D2Q9 lattice with nine discrete velocities. The velocity vectors are illustrated in Figure 2.

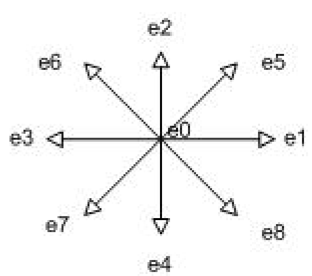

Figure 2. The nine-speed square lattice used in the lattice Boltzmann simulations. (After Guo *et al*, 2000)

The velocity directions of the D2Q9 Lattice Boltzmann BGK model are defined as (Guo *et al*, 2000).

$$e_i = \begin{cases} (0,0) & i=0 \\ (\cos[(i-1)\pi/2], \sin[(i-1)\pi/2]) & i=1,2,3,4 \\ \sqrt{2}(\cos[(i-5)\pi/2+\pi/4], \sin[(i-5)\pi/2+\pi/4]) & i=5,6,7,8 \end{cases} \quad (3)$$

Let $f_k(x,t)$ be a non-negative real number describing the distribution function of the fluid density at site *x* and time *t* moving with velocity e_k towards the neighboring lattice site located at x+ e_k, where the subscript *k* refer to the velocity direction (*k*=1,…,9). The distribution functions evolve according to the Boltzmann equation that is discrete in both time and space.

$$f_k(x+e_k, t+1) = f_k(x,t) + \Omega_k(x,t) \quad (4)$$

Where $\Omega_k(x,t)$ is the collision operator representing the rate of change of the particle distributions due to collisions (Kumar *et al*, 1999). Collection of particles of unit mass and unit momentum moves on the lattice. Mass and momentum of the particles are locally conserved after collision of the particles.

The fluid density ρ and velocity u are obtained from the density distribution function $f_k(x,t)$:

$$\rho = \sum_k f_k \quad (5)$$

$$\rho \mathrm{u} = \sum_k f_k e_k \quad (6)$$

As it is stated in (Wolf-Gladrow, 2000) at macroscopic scale the behavior of these particles is the same as that is predicted by the incompressible Navier-Stokes equations.

Boundary Conditions

A boundary condition with a constant pressure difference is used at inlet and outlet of the fracture aperture, where all fluid densities are propagated from non-occupied nodes along the lattice-connection lines to their next neighbors. The physical boundary condition at solid-fluid interfaces is the no-slip boundary condition, which in LBM is usually realized as bounce-back rule. This is physically appropriate whenever the solid wall has a sufficient rugosity to prevent any net fluid motion at the wall (Succi, 2001). The complete bounce-back scheme is used to simulate the no-slip boundary condition, which requires that when a particle distribution streams to a solid boundary node, it scatters back to the node it came from. The velocity vector of all fluid densities is inverted, so all the fluid densities will be sent back to the node where they were located before the last propagation step, but with opposite velocity vector.

Algorithm

There are many different algorithms available for implementing LBM. The following pseudo code shows how LBM was implemented in Matlab V 7.0 in this study (Keehm, 2003).

```
Start Program
Read in Obstacle Location File
Set initial density distribution
Loop for T time Steps
{
        Redistribute along first lattice column
        Propagate fluid particles
        Check for obstacle (bounce-back)
        Calculate density and velocity from Eqn 5 & 6
        Calculate permeability
        If((new perm-old perm) < tolerance_value))
exit loop
}
Write velocity data to file
End
```

2.2 Synthetic Fractures

It is very important to understand the fluid flow through natural fractures in rocks. The geometry of the fracture surfaces affects the hydraulic properties of the fractured rock. Roughness at the surface of the fractures could be described efficiently by using the fractal geometry concepts (Feder, 1988). Since studying rough, anisotropic fractures in the laboratory is difficult synthetic fractures could be used. Synthetic fracture is the term used to describe fractures that are created numerically in such a way that they share the same mean geometrical characteristics as specific natural fractures measured by profiling and then tuning (Glover, *et al*, 1998). For example numerical synthetic fractures can be created from unmatched fractal surfaces (Amedei *et al*, 1994). Geostatistical techniques like conventional kriging and conditional simulation (Deutsch and Journel, 1992) could also be used to create synthetic fractures. In this work numerical modeling is used to simulate fluid flow in synthetic rock fractures that share the same physical properties with the natural fractures. In our work SynFrac software is used to create synthetic fractures (Glover *et al*, 1998). This software uses modified methods for producing synthetic rough surfaces whose geometric properties are tuned to mimic natural fractal surfaces in rocks in order to create synthetic fractures that are statistically identical to those found in rocks.

3 FRACTURE GENERATION AND FLOW SIMULATION

In this section methodologies used both for synthetic fracture generation and the simulation of the fluid flow in these fractures will be defined.

3.1 Synthetic Fracture Generation

SynFrac software originally generates three-dimensional fractures. The resolution of the fracture can be altered with in the range from 64x64 to 1024x1024. In addition to resolution, parameters like fractal dimension or anisotropy factor could be altered to generate fractures that have the same resolution but different physical properties. Fractal dimension for each surface is a value between 2 and 3; this value determines the roughness of the fracture surface. Another parameter that is altered is the anisotropy factor, which is used to generate anisotropic synthetic fractures. As the anisotropy factor deviates from unity all the scales in one direction along the fracture surface will be greater than the scales in other direction. A sample fracture surface created by SynFrac is given in Fig 3 (Glover *et al*, 1998).

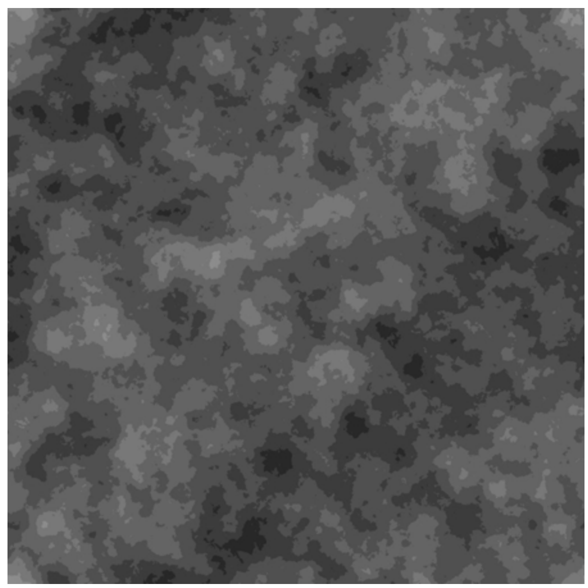

Figure 3. Fracture aperture distribution created by SynFrac. Blacks are low aperture areas.

As the lattice Boltzmann simulation is performed at two-dimensions, 2D slices are obtained from the 3D fracture apertures. Figure 4 shows a 2D fracture aperture obtained by slicing the three-dimensional fracture for a given plane.

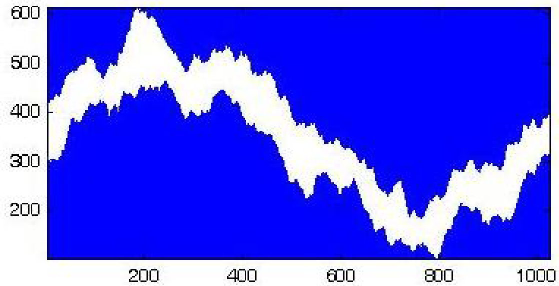

Figure 4. Two dimensional fracture aperture obtained by slicing.

This sliced two-dimensional fracture forms the basis for our lattice Boltzmann simulation. SynFrac software outputs the heights of the top and bottom surfaces of the created fracture, an instance of the output data is shown in Table 1. This data is then converted into binary format (1's and 0's) in order to be used with lattice Boltzmann algorithm. This process is illustrated in Fig 5, where 1's represent grains and 0's represent pore space. In order to increase accuracy of the simulation synthetic fractures are created at maximum resolution (1024). Resolution of the fracture is, 1024 in x-direction and a value which is determined according to the min-max value of the bottom and top in y-direction changes between 500 and 700.

Table 1. Sample 2D fracture data.

X-Loc	Y-Loc	Top (mm)	Bottom (mm)	Aperture (mm)
1	103	4.879	4.140	0.738
1	104	4.852	4.151	0.701
1	105	4.848	4.165	0.683
1	106	4.856	4.165	0.691
1	107	4.828	4.193	0.636
1	108	4.812	4.216	0.596

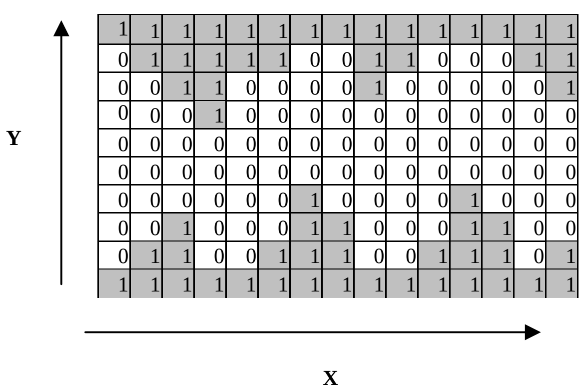

Figure 5. Binary representation of two-dimensional fracture aperture.

3.2 Lattice Boltzmann Simulation of Fluid Flow in Fractured Geothermal Reservoirs

Fractal dimensions of the fracture patterns of some geothermal reservoirs (Kizildere and Germencik) located in south western Turkey was used to generate synthetic fractures (Babadagli, 2001; Babadagli, 2002). Fractal dimensions obtained by applying methods like box counting from aerial photographs, outcrops and thin sections ranged from 2.21 to 2.50 (Table 2).

Table 2. Results of the lattice Boltzmann simulations for different fractal dimensions.

Fractal Dimension	Mean Aperture (mm)	LB-Perm (md)
2.21	1.3443	1.59E+06
2.25	1.4550	1.68E+06
2.30	1.6051	1.81E+06
2.32	1.6691	1.86E+06
2.35	1.7693	1.94E+06
2.38	1.8746	2.02E+06
2.40	1.9478	2.05E+06
2.45	2.1411	2.18E+06
2.47	2.2224	2.23E+06
2.50	2.3486	2.29E+06

Simulations (Table 3) were performed in order to understand the effects of the parameters during the fracture generation phase to the absolute permeability of the fractures. At each step synthesized fracture with its fractal dimension or anisotropy factor was changed, converted into binary format and used as an input for the lattice Boltzmann simulation. Velocity vectors on each grid point were calculated by the lattice Boltzmann method (Fig 6). Absolute permeability k of the fracture could then be obtained by calculating the mean flux from the velocity vectors and with the Darcy's law.

$$\langle q_x \rangle = \frac{k}{\mu}\frac{dP}{dx} \qquad (7)$$

Where μ is the dynamic viscosity of the fluid and $\langle q_x \rangle$ is the volumetric average of fluid flux.

Table 3. Parameters used in the LBM simulations for different fractal dimensions, anisotropy factors and mismatch lengths.

Resolution	1024
Physical size (mm)	100.00
Transition length (mm)	10.00
Standard deviation (mm)	1.00
Max matching fraction	1.00
Min matching fraction	0.00

Permeability values obtained by LBM are compared by the empirical results that are calculated by using Eqn 1 without or with roughness. Moreover, permeability is estimated from the following equation (Zhang *et al*, 1996):

$$k \approx \delta^{\beta} \qquad (8)$$

Where δ is mean fracture aperture and β is an exponent.

4 RESULTS OF THE LATTICE BOLTZMANN SIMULATION

The method was first verified for pipe flow using Hagen-Poiseuille law. It was observed that the difference between the results were less than %0.09. Then several runs were conducted to identify flow velocity patterns. Synthetic 2D fractures were selected from the same location in 3D. That's why the fracture geometry was similar but the rugosity was somewhat different for each case (Fig 6). Thus, the fracture sloped upwards first following a downhill that ended with increasing slope. It was observed that for a constant pressure gradient the highest velocity was observed near the inlet of the fracture corresponding to locations where the aperture was significantly lower than the rest of the fracture. Then the high velocity flow dissipated near the end of the fracture for all cases. For constant anisotropy factor, as the fractal dimension increased (from 2.21 to 2.5 corresponding to %13 increase) the magnitude of the highest velocity observed increased (approximately %30). On the other hand, as the anisotropy factor increased from 1 to 3, the location of highest velocities along the fracture changed. Moreover, the magnitude of the highest velocity decreased. As the mismatch length increased mean fracture aperture increased and thus the permeability increased (Fig. 7). The magnitude of the highest velocity observed along the fracture couldn't be correlated.

Simulations were then conducted to understand the effect of fractal dimension and anisotropy factor to fracture permeability. While creating synthetic fractures each of these parameters was altered and other parameters were held constant. Table 2 shows the result of the LBM permeability calculations for different fractal dimension values. Figure 8 shows permeability values that are calculated by LBM vs. mean aperture – fractal dimension ratio. The fracture permeability increases linearly with a high correlation coefficient as the mean aperture fractal dimension ratio increases. LBM fracture permeabilities were two orders of magnitude lower than the permeabilities obtained from the cubic law (Eqn 2). This suggests that for a rough self-affine fracture one may have a fractal dimension dependent exponent that is larger than 2. Our simulations suggest an exponent range from 4.27 to 5.66 that are in accord with the range (2 to 6) provided by Zhang *et al* (1996). Moreover, for anisotropy equal to 1, there is a linear relationship between the fractal dimension D and the exponent given by the following equation:

$$\beta = 4.8065D - 6.4154 \qquad (9)$$

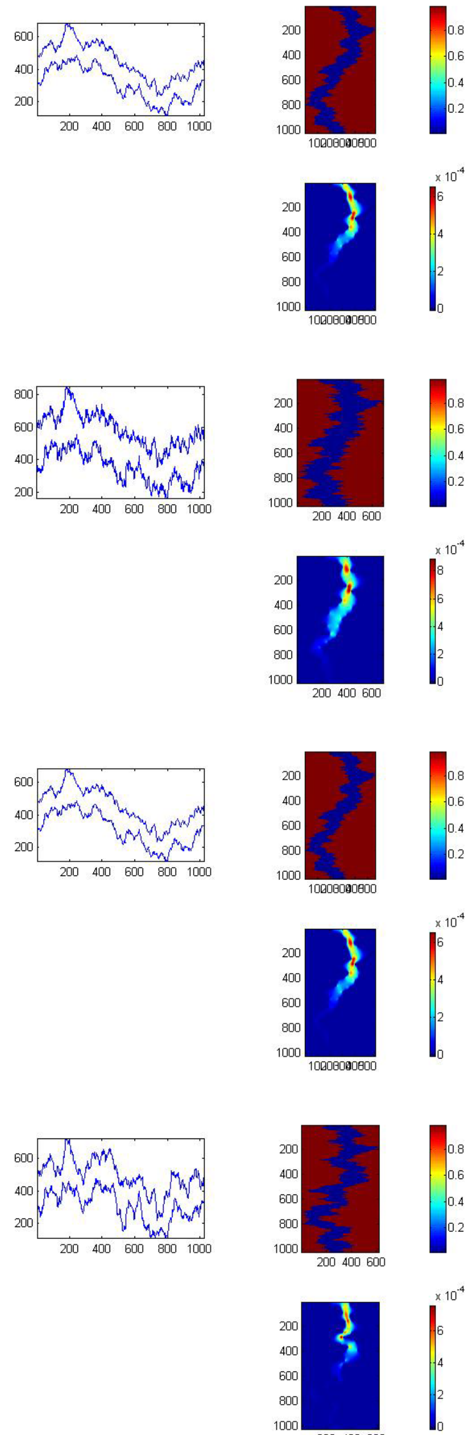

Figure 6. Generated fracture aperture and velocity distribution for fractal dimension and anisotropy factor values top to bottom (2.21 and 1.0), (2.5 and 1.0), (2.25 and 1.0), (2.25 and 3.0).

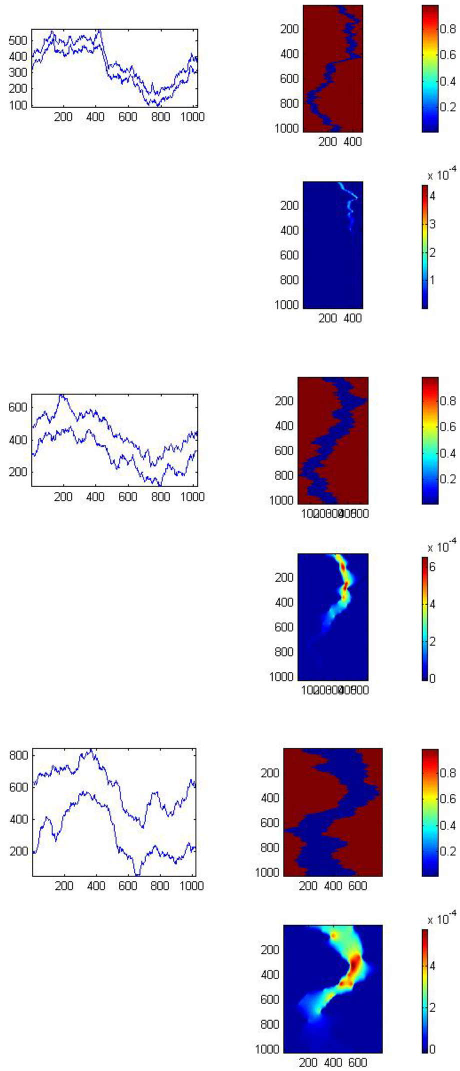

Figure 7. Generated fracture aperture and velocity distribution for mismatch length of 5, 15 and 25 mm.

Another set of simulations was performed to understand the effect of the changes in anisotropy factor to the fracture permeability. Anisotropy factor is a ratio of the wavelengths in each direction. If anisotropy factor is less than 1 anisotropy is transverse to x direction; however, if anisotropy factor is more than 1 anisotropy is transverse to y direction (Glover *et al*, 1998). As the anisotropy factor increased from 1 to 3, permeability decreased (Table 3). Similar results are reported in the literature for self-affine fractures (Madadi and Sahimi, 2003). When permeability values are plotted against anisotropy factors a second-order polynomial relationship was observed (Fig 9). It was observed that for a given fractal dimension, anisotropy and exponent relationship is linear. For example for D equals to 2.25 the following relationship was observed.

$$\beta = 0.5063*A + 3.8642 \qquad (10)$$

Where A is anisotropy factor.

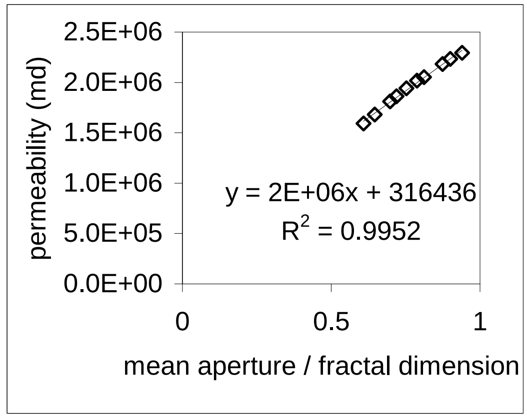

Figure 8. Relationship between LBM permeability and mean aperture-fractal dimension ratio.

Table 3. Permeability values of the fractures for different anisotropy factors.

Anisotropy Factor	LB-Permeability (md)
1,00	1,68E+06
1,20	1,60E+06
1,30	1,56E+06
1,35	1,53E+06
1,40	1,51E+06
1,50	1,46E+06
1,60	1,42E+06
1,80	1,33E+06
2,50	1,21E+06
3,00	1,15E+06

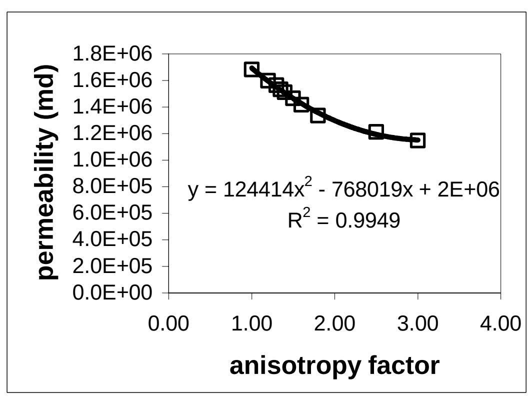

Figure 9. Relationship between LBM permeability and anisotropy factor.

The final parameter that affects fracture permeability is mismatch length. It was shown previously that natural fractures are correlated to some degree at long wavelengths but at short wavelengths the surfaces are not identical (Brown, 1995). These two different behaviors are modeled by a critical wavelength called the mismatch length. Above this length the fracture surfaces are correlated but below it the fractures behave independently. In our simulations, as the mismatch length increased the fracture surfaces became correlated and smoother for a given fractal dimension. The mean aperture also increased. This results in an increase in permeability. A linear relationship was observed with mismatch length and the LBM permeability (Fig 10).

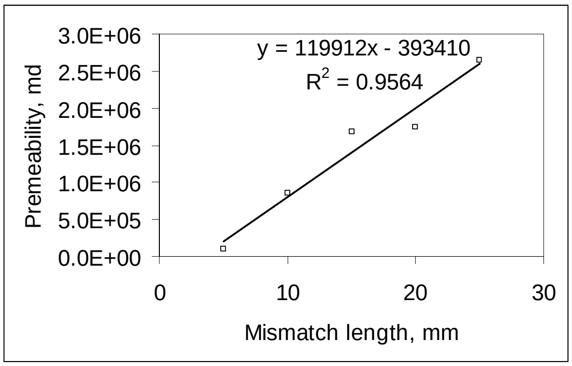

Figure 10. Relationship between LBM permeability and mismatch length.

In order to generalize the findings, simulations that cover a wide range of fractal dimensions, anisotropy factors, mean fracture apertures and mismatch lengths need to be conducted. However, it is not possible to cover all parameters within a reasonable time frame. In order to tackle this problem artificial neural network (ANN) technology was used (Fig 11). Back propagation technique (Rumelhart *et al*, 1986) and 71 different LBM simulations were used to train different artificial neural networks and the best performing network was selected (Table 4). ANN input parameters consisted of fractal dimensions, anisotropy factors, average mean apertures and fracture porosities and LBM permeability is selected as ANN output. Approximately %10 of the input data was held for validation purposes. Since there were several orders of magnitude difference between the input data the LBM permeability was scaled to values between 0 and 1 by dividing the LBM permeabilities to maximum calculated permeability ($2.29x10^6$ md). It was observed that the mean square errors were less than %0.71 for the validation data set (Fig 12). Using the trained ANN several runs were conducted to check the aforementioned results.

Table 4. ANN model properties.

Input nodes	4
Output nodes	1
Hidden layer 1	20
Hidden layer 2	8
Momentum factor	0.1
Learning parameter	0.2

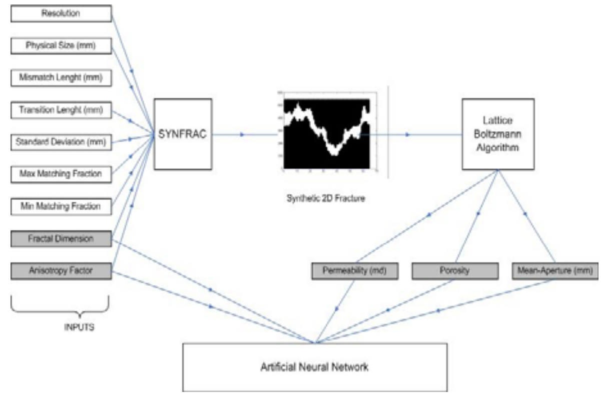

Figure 11. Architecture for LBM simulation and artificial neural network training.

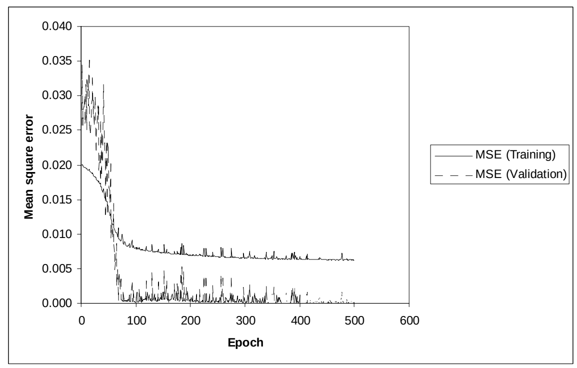

Figure 12. Mean square errors observed for artificial neural network training and validation data sets.

The ANN results confirmed the aforementioned findings (Fig 13). For example the second order relationship observed between the anisotropy factor and LBM permeability was obtained for all fractal dimensions. One of the advantages of using the ANN technology is that one can establish the importance of parameters that influence a process. For a given average fracture aperture it was observed that the as anisotropy factor increased from 1 to 3 the permeability decreased %62 and %75 for low and high fractal dimensions respectively. On the other hand, for a given mean fracture aperture, the fractal dimension change from 2.25 to 2.35 resulted in approximately %1.8 to %5.2 change in permeability. It was also observed that as the anisotropy factor increased from 1 to 3 the change in permeability decreased as the fractal dimension or mean fracture aperture increased. Thus it could be concluded that as the fracture rugosity increases mean fracture aperture and fractal dimension do not dominate the permeability change anymore.

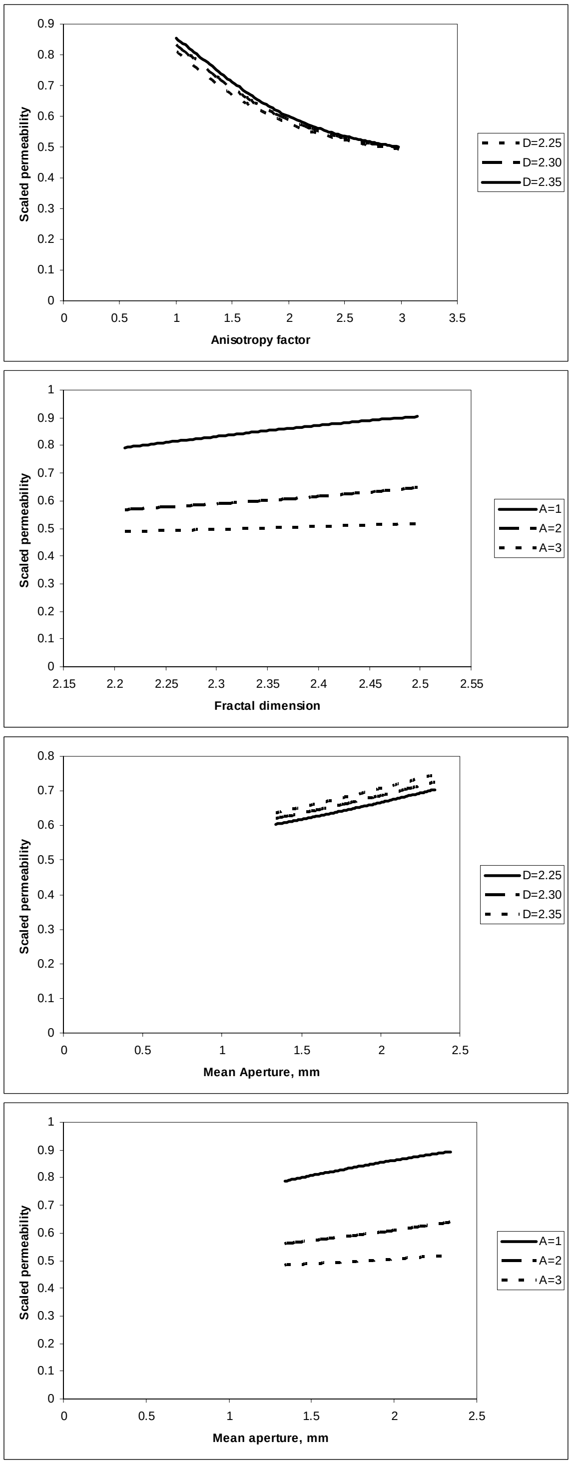

Figure 13. ANN results. Permeability anisotropy factor, mean fracture aperture and fractal dimension relationships.

5 CONCLUSIONS

Lattice Boltzmann Method was used to obtain fracture permeabilities of synthetic fractures created using a fractal technique. For the fractal geothermal reservoirs located in South West Turkey it was observed that velocity increased at locations where the fracture aperture decreased along the fracture. There is a linear relationship between permeability and mean aperture – fractal dimension ratio as well as the mismatch length. However, the relationship is second order for anisotropy factor. A neural network trained using the LBM simulations showed that anisotropy of the fracture has more influence on the fracture permeability than the fractal dimension and the mean fracture aperture. Thus the fracture geometry is important.

REFERENCES

Amedei, B., Illangsekare, T., “A Mathematical Model for Flow and Transport in Non-Homogeneous Rock Fractures”, Int. J. Rock Mech. Min. Sci. Geomech. Abstr., 31, 719-731, (1994).

Amyx, J., Bass, D., Whiting, R., “Petroleum Reservoir Engineering”, (1960).

Bear, J. “Dynamics of Fluids in Porous Media”, American Elsevier Publishing Co., New York: 764 pp., (1972).

Babadagli T “Fractal analysis of 2-D fracture networks of geothermal reservoirs in south-western Turkey” J VOLCANOL GEOTH RES 112 (1-4): 83-103 DEC (2001).

Babadagli T “Scanline method to determine the fractal nature of 2-D fracture networks” MATH GEOL 34 (6): 647-670 AUG (2002).

Brown, S.R. “Simple mathematical model of a rough fracture” J. Geophys. Res. 100, 5941-5952, 1995.

Deutsch C. V. Journel, A. G. “GSLIB: Geostatistical Software Library and User's Guide”, Oxford University Press, New York, (1992), 61-116.

Feder, J., “Fractals”, Plenum Press, NY, 283 pp, (1988).

Frisch, U., Hasslacher, B., Pomeau, Y., “Lattice Gas Automata for the Navier-Stokes Equations”, Phys. Rev. Lett. 56, 1505, (1986).

Glover, P. W. J., Matsuki, K., Hikima, R., Hayashi, K., “Synthetic Rough Fractures in Rocks”, Journal of Geophysical Research 103, B5, 9609-9620, (1998).

Golf-Racht, Van, T. D, “Fundamentals of Fractured Reservoir Engineering”, Elsevier Publishing Company, 710 pp (1982).

Guo, Z., Shi, B., Wang, N., “Lattice BGK Model for Incompressible Navier-Stokes Equation”, Journal of Computational Physics 165, 288-306, (2000).

Ilachinski A., “Cellular Automata, a Discrete Universe”, World Scientific Publishing Company; 1st edition, 840 pp, (2001).

Keehm, Y., “Computational Rock Physics: Transport Properties in Porous Media and Applications”, Phd Thesis, Stanford University Department of Geophysiscs, (2003).

Kumar, R., Sriram, S., Nivarthi, H., Davis, T., Kroll, D. M., Maier, R. S., “Application of the Lattice-Boltzmann Method to Study Flow and Dispersion in Channels with and without Expansion and Contraction Geometry”, Int. J. Numer. Meth. Fluids 31: 801-819, (1999).

Lomize, G.M. “Flow in fractured rocks” (In Russian), Gosenergoizdat, Moscow: 127 pp, (1951).

Louis, C.A. “A study of groundwater flow in jointed rock and its influence on the stability of rock masses”, Rock Mech. Res. Rep. 10, Imperial College, London: 90 pp., (1969).

Madadi, M., Sahimi, M. “Lattice Boltzmann simulation of fluid flow in fracture networks with rough, self-affine fractures”, Physical Review E, 67, 026309, (2003).

McNamara, G., Zanetti, G., “Use of the Boltzmann Equation to Simulate Lattice-Gas Automata”, Phys. Rev. Lett. 61, 2332-2335, (1988).

Rumelhart, D. E., Hinton, G. E., and Williams, R. J., 1986. Learning representations by back-propagating errors. Nature, 323, 533-536.

Snow, D.T. “Anisotropic permeability of fractured media”, Water Resources Research, 5 (6): 1273-1289, (1965).

Succi, S., Foti, E., Higuera, F., “Three-dimensional flows in complex geometries with lattice Boltzmann method”, Europhysics Letters, 10(5): 433-438, (1989).

Succi, S., “The Lattice Boltzmann Equation for Fluid Dynamics and Beyond”, Oxford University Press, 368 pp (2001).

Withersphoon, P. A., Wang, J. S. Y., Iwai K., Gale, J. E., “Validity of the cubic law for fluid flow in a deformable rock fracture”, Water Resources Research, 16, 6, 1016 (1980).

Wolfram, S., “Universality and Complexity in Cellular Automata”, Physica D, 10, 1-35, (1984).

Wolf-Gladrow, D., “Lattice-Gas Cellular Automata and Lattice Boltzmann Models”, Springer-Verlag Telos, 308 pp, (2000).

Zhang, X., Knackstedt, M.A., Sahimi, M. “Fluid flow across mass fractals and self-affine surfaces”, Physica A, 233, 835, (1996).